

Ya. Saliy<sup>1</sup>, L. Nykyruy<sup>1</sup>, G. Cempura<sup>2</sup>, O. Soroka<sup>3</sup>, T. Parashchuk<sup>2</sup>, I. Horichok<sup>1</sup>

## Periodic nanostructures induced by point defects in $\text{Pb}_{1-x}\text{Sn}_x\text{Te}$

<sup>1</sup>Vasyl Stefanyk Precarpathian National University, Ivano-Frankivsk, Ukraine, [ihor.horichok@pnu.edu.ua](mailto:ihor.horichok@pnu.edu.ua)

<sup>2</sup>AGH University of Science and Technology, Krakow, Poland

<sup>3</sup>Ivano-Frankivsk National Medical University, Ivano-Frankivsk, Ukraine

Lead tin telluride solid solutions are excellent candidates for the *p*-type conduction legs of the thermoelectric generator modules. The investigation of their microstructure properties is an important issue, that can effectively modify their electronic and thermal transport properties. In this work, we show the experimental dependences of the  $\text{Pb}_{1-x}\text{Sn}_x\text{Te}$  component distribution, which were identified as periodic nanostructures with an amplitude of  $\lambda \approx 50\text{-}500$  nm. The observed periodicity is explained by the generation and recombination of point defects due to diffusion processes during the synthesis, sintering, and annealing of samples. A model describing the formation of such inhomogeneities in  $\text{Pb}_{1-x}\text{Sn}_x\text{Te}$  ternary alloys during isothermal annealing is proposed.

**Keywords:** point defects, nanostructures,  $\text{PbSnTe}$ .

Received 17 September 2022; Accepted 19 February 2023.

## Introduction

Lead telluride-based compounds are among the best materials for medium-temperature thermoelectric applications [1-4]. The electronic and thermal transport properties of these materials can well-tuned using the point defects and nano-inclusions [5-8]. However, a much more interesting effect is the formation of the self-organized nano-inclusions, which may have a significant effect on the physical properties. Particularly, the formation of periodic structures was observed in  $\text{PbS}$ ,  $\text{PbSe}$ , and  $\text{PbTe}$  thin films grown by the thermal deposition method [8-11]. The observed changes of the Seebeck coefficient  $S(d)$  and electrical conductivity  $\sigma(d)$  at minima and maxima of the thickness dependences of the film were up to  $\sim 2$  times. The authors associated this periodicity ( $\Delta d \approx 30$  nm) with the dimensional quantum effect. However, if the amplitude of oscillations at the level of ten nanometers can still be explained by the dimensional quantum effect, the value of  $\Delta d$  at the level of hundreds of nanometers is questionable. In particular, in ref. [11], an increase in the electron concentration by  $\sim 2$  times leads to a decrease in the period of oscillations also by  $\sim 2$  times (from 200 to 100 nm), which is 5 times higher than the values estimated from the quantization

conditions.

The organization of periodic nanostructures not for film material, but bulk  $\text{CdHgTe}$  crystals, was established in ref. [12]. The authors claimed that the period of oscillation can vary from nanometers to micrometers. The main factor influencing this value is the absolute values and the ratio between concentrations of vacancies and interstitial atoms. The concentration of interstitial atoms may be several orders of magnitude lower than the concentration of vacancies. Therefore, the interstitial atoms, practically without affecting the properties of the material, determine the periodicity of vacancy distribution, which in turn determines the periodicity of nanostructures in the material. Other factors, i.e. the nature of the initial inhomogeneities in material, are less important.

Herein, in the case of the  $\text{PbTe}$ -based materials, we developed a model, which suggests that the carrier concentration is the main parameter to control the periodicity of the formed nanostructures. By tuning the carrier concentration of  $\text{Pb}_{1-x}\text{Sn}_x\text{Te}$  by I-doping we were able to establish the periodic structure of the material with an amplitude  $\lambda \approx 50\text{-}500$  nm, which is confirmed by TEM analysis.

## I. Experimental section

### Synthesis and characterization of materials

Materials were synthesized in quartz ampoules evacuated to a residual pressure of  $10^{-5}$  mbar. The ampoules were subjected to rigorous purification, which included washing in a  $1\text{HNO}_3:3\text{HCl}$  concentrated acid mixture and frequent cleaning with distilled water and isopropanol. Polycrystalline  $\text{Pb}_{1-x}\text{Sn}_x\text{Te}_{1-y}\text{I}_y$  materials were synthesized by melting Pb (99.999%), Te (99.999%), Sn (99.99%), and  $\text{PbI}_2$  (99.999%) at 1273 K. Each ampoule was shaken at the liquid state to force the mixing of the components and then taken from the furnace and quenched in cold water. The obtained ingots were crushed into a fine powder via hand milling in an agate mortar and then densified using the spark plasma sintering technique at 873 K for 20 min in a 10 mm diameter graphite mold under axial compressive stress of 50 MPa in an argon atmosphere. The heating/cooling rate was 50 K/min. For homogenization, all samples were annealed for 20 hours at 873 K in an argon atmosphere.

The structural analyses of the samples were studied using X-ray diffractometer STOE STADI P (by STOE & Cie GmbH, Germany) according to the modified Guinier geometry scheme using the transmission mode ( $\text{CuK}\alpha_1$ -radiation, concave Ge-monochromator (111) of the Johann type;  $2\theta/\omega$ -scan, angle interval  $10.000^\circ \leq 2\theta \leq 85.000^\circ$  with the step of scanning of  $0.015^\circ$ ; the scan time in step 100-230 s). The initial processing of experimental diffraction arrays was performed using PowderCell (version 2.4) software packages.

For SEM and EDX analyses, the samples were embedded in conductive resin, and subsequently polished, using  $0.1 \mu\text{m}$  diamond powder in a slurry. The analysis of the samples' chemical composition was carried out using a scanning electron microscope (JEOL JSM-6460LV Scanning Electron Microscope) equipped with energy-dispersive X-ray spectroscopy capabilities.

The specimen for TEM investigations was prepared

with the FIB technique. For TEM investigations, Titan Cubed G2 60-300 (FEI), a probe Cs-corrected (S)TEM was used. The microscope was equipped with the ChemiSTEM EDX system based on four windowless Silicon Drift Detectors (Super X). Phase identification based on Selected Area Electron Diffraction (SAED) patterns was performed using JEMS v4.7830 software (Pierre Stadelmann, JEMS-SAS, Switzerland).

## II. Results and discussion

Fig. 1a presents powder X-ray diffraction patterns of pristine PbTe,  $\text{Pb}_{0.7}\text{Sn}_{0.3}\text{Te}$ , and  $\text{Pb}_{0.7}\text{Sn}_{0.3}\text{Te}_{0.99}\text{I}_{0.01}$  solid solutions, normalized to the most intense (200) reflection. XRD results prove that all alloys have a structure of cubic PbTe. The estimated compositional dependence of the lattice parameter  $a$  for  $\text{Pb}_{1-x}\text{Sn}_x\text{Te}$  agrees well with Vegard's law, as was already observed in earlier works [13].

SEM analysis of sintered samples (Fig. 1b) shows that there are no large macro defects, in particular, micrometer-sized pores, indicating the high homogeneity of the sample. This conclusion is also confirmed by the density measurements. In particular, for the  $\text{Pb}_{0.7}\text{Sn}_{0.3}\text{Te}_{0.99}\text{I}_{0.01}$  sample, the value of  $\rho$  determined by the Archimedes method was equal to 99% compared with the theoretical XRD density.

The investigation of the structure using TEM indicates the presence of periodic formations (Fig. 2). The distance between them is up to 100 nm. The fact that the formation of these inclusions is caused by periodicity in the distribution of components is confirmed by the quantitative chemical composition analysis using EDX (Fig. 3-4). It is important to note that these inhomogeneities are not inclusions of another phase. Their crystal structure is similar to the structure of the matrix material.

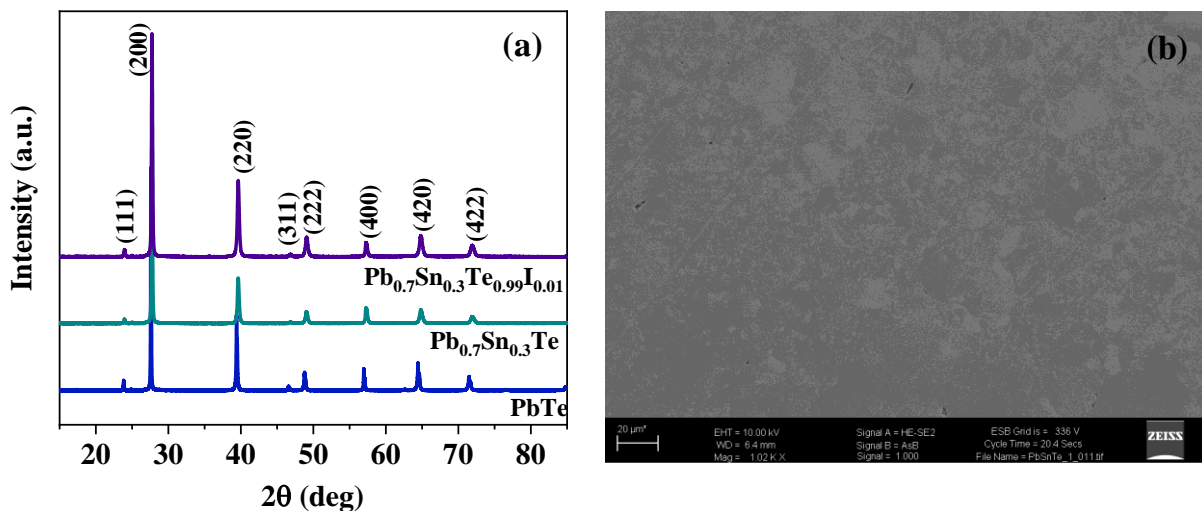


**Fig 1.** (a) The powder X-ray diffraction patterns for PbTe,  $\text{Pb}_{0.7}\text{Sn}_{0.3}\text{Te}$ , and  $\text{Pb}_{0.7}\text{Sn}_{0.3}\text{Te}_{0.99}\text{I}_{0.01}$  specimens; (b) the Scanning Electronic Microscopy image for the representative  $\text{Pb}_{0.7}\text{Sn}_{0.3}\text{Te}_{0.99}\text{I}_{0.01}$  sample.

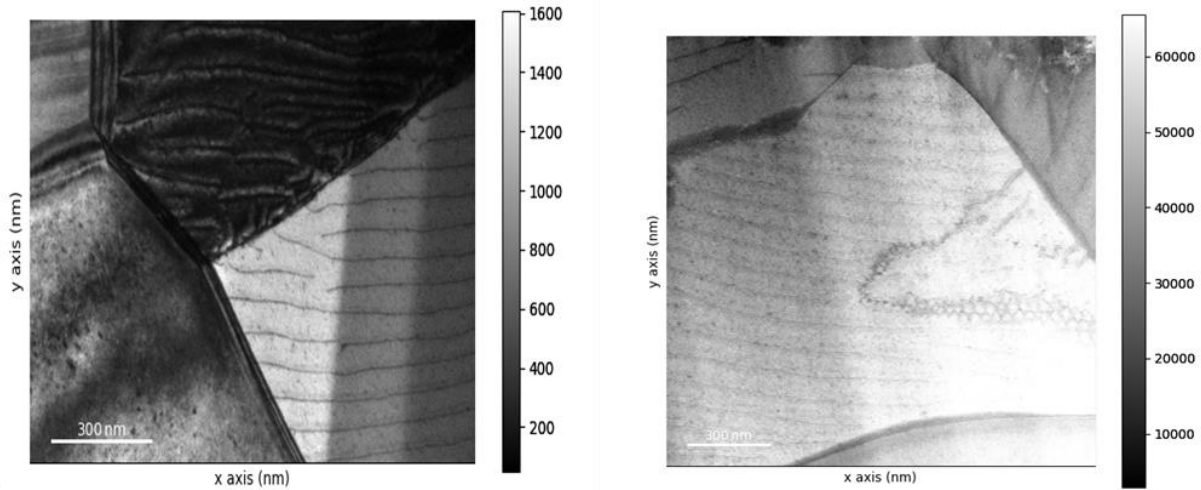


**Fig. 2.** Transmission electronic microscopy image of the  $p\text{-Pb}_{0.7}\text{Sn}_{0.3}\text{Te}_{0.99}\text{I}_{0.01}$  specimen after spark plasma sintering.

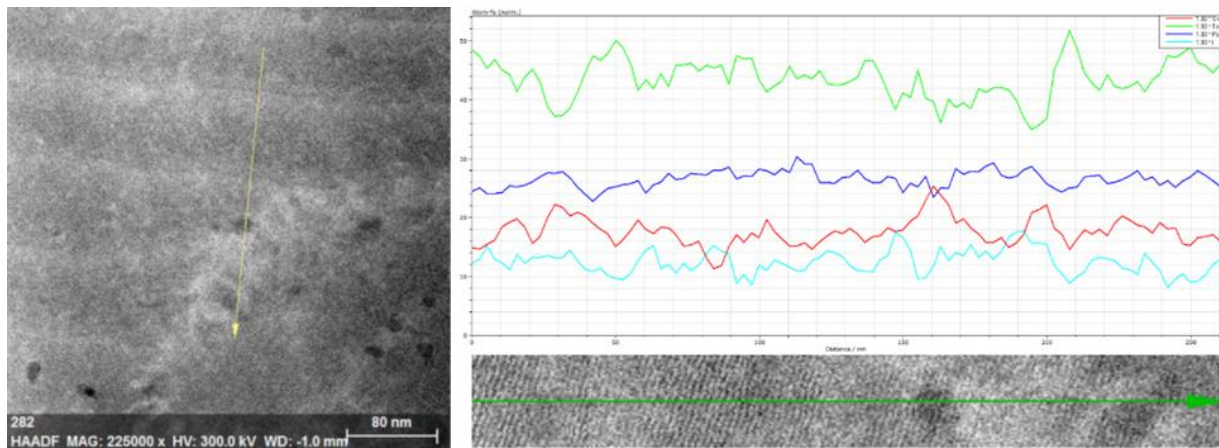


**Fig. 3.** EDX line scan for the  $\text{Pb}_{0.7}\text{Sn}_{0.3}\text{Te}$  specimen after spark plasma sintering.

According to the EDX analysis data presented in Fig. 3, the Fourier analysis was performed. The results are shown in Fig. 4. It can be seen from the calculations that the distribution of the components of the solid solution along the direction of the quantitative elemental analysis has a well-defined periodic character. The theoretically determined oscillation period for tin and tellurium is approximately the same ( $\approx 42$  nm), for lead, it is somewhat larger, but of the same order ( $\approx 50$  nm). The most important thing here is that the distributions of Te and Sn are in antiphase with each other.

It is worth noting that the 1/3 part of the line along which the analysis was carried out is located at the grain boundary. In addition, in this area, a contrasting area is observed, which, according to elemental analysis, is enriched with tin and, accordingly, with a reduced content of lead and tellurium. This explains the slightly more intense oscillations in the concentration of components in this area. It is also important that a satisfactory correlation between the modeled curve and experimental ones was achieved when taking into account two harmonics - the main one, which almost completely determines the main characteristic features of the experimental dependence, and the additional one, which leads to some improvement of the corresponding correlation. Such a regularity may indicate the possibility of the existence of several (at least

two) factors that determine the periodic distribution of components in a solid solution. Moreover, one of them is dominant.

#### Model for diffusion instability of tellurium atoms distribution in $\text{Pb}_{1-x}\text{Sn}_x\text{Te}$

The essentially nonlinear nature of mutual diffusion processes in the ternary alloys results in the inhomogeneity of the distribution of components and defects [14]. A theoretical model describing the formation of the periodic distribution of mercury atoms in  $\text{Cd}_{1-x}\text{Hg}_x\text{Te}$  during post-growth cooling is proposed in ref. [12, 15]. The mechanism of phenomena is based on the diffusion instability in a system containing vacancies and interstitial atoms. It was estimated, that if the initial concentration of interstitial mercury atoms is higher than some limit value of  $3 \times 10^{17} \text{ cm}^{-3}$  for  $\text{Cd}_{0.8}\text{Hg}_{0.2}\text{Te}$  at long-time annealing ( $T=473$  K), the periodic distribution of mercury atoms appears from the insignificant fluctuation. The spatial and temporal scale of the distribution is determined by the equilibrium concentration of vacancies and does not depend on the specific type of fluctuation. The period increases from 10 nm to 3000 nm with a decrease in the equilibrium concentration of vacancies from  $10^{19}$  to  $10^{14} \text{ cm}^{-3}$ . At low concentrations, the formation of the periodic structures takes a much longer

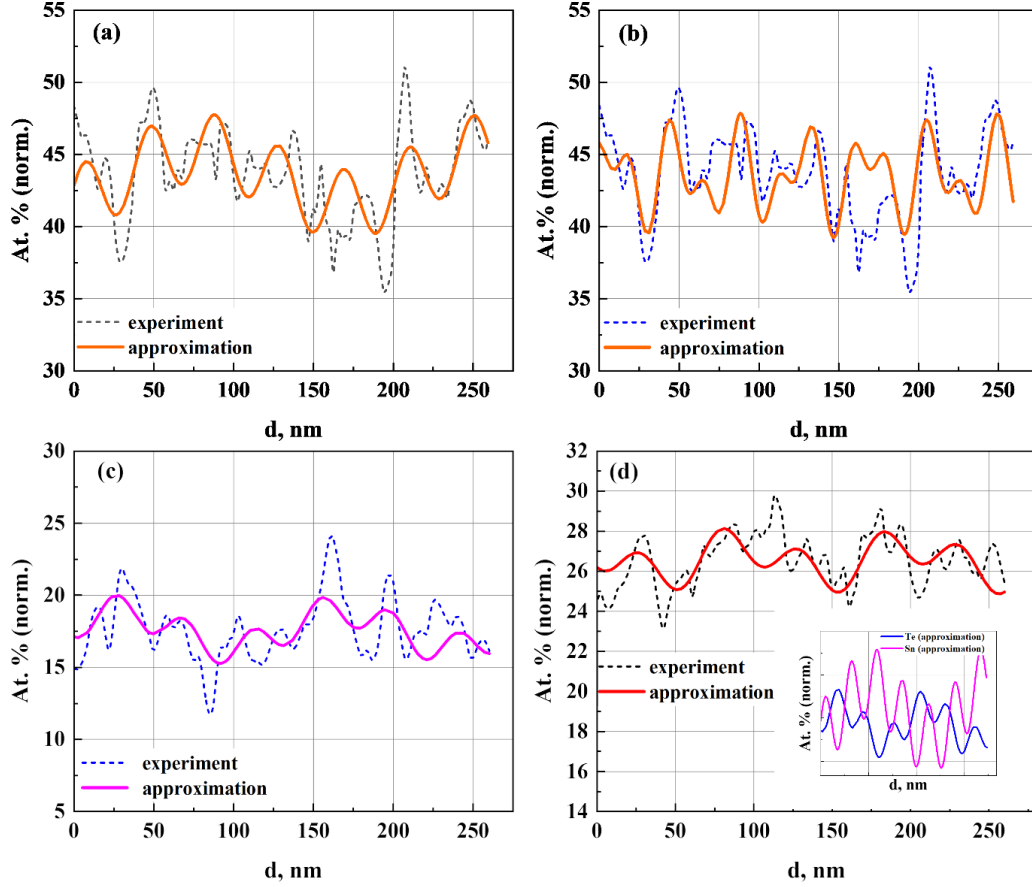


**Fig. 4.** The element distribution along the EDX line scanning. The dashed line indicates the experimental measurements, the solid lines indicate the simulation using the sinusoidal function. (a) – Te distribution (the main harmonic  $\lambda = 40.3$  nm, the amplitude  $p_a = 2.4$  at. %, the second harmonic  $\lambda = 185$  nm); (b) – Te distribution (the main harmonic  $\lambda = 40.3$  nm, the amplitude  $p_a = 2.4$  at. %, the second harmonic  $\lambda = 23$  nm); (c) Sn distribution (the main harmonic  $\lambda = 42.8$  nm, the amplitude  $p_a = 1.1$  at. %, the second harmonic  $\lambda = 138$  nm); (d) Pb distribution (the main harmonic  $\lambda = 50.9$  nm, the amplitude  $p_a = 1.0$  at. %, the second harmonic  $\lambda = 106.9$  nm). The inset shows that distributions of Te and Sn are in antiphase with an almost identical oscillation period of  $41.5 \pm 1.2$  nm.

time.

Considering the concentration of free charge carriers, we can assume that the  $p\text{-Pb}_{0.7}\text{Sn}_{0.3}\text{Te}_{0.99}\text{I}_{0.01}$  semiconductor possesses a concentration of lead acceptor vacancies  $V_0 = 2 \times 10^{19} \text{ cm}^{-3}$  and donor interstitial lead atoms  $I_{\text{Pb}} = 10^{18} \text{ cm}^{-3}$ . This material has a crystalline structure of the NaCl type with a lattice constant  $a = 6.4611 \text{ \AA}$  [16], and therefore the concentration of the metal atoms is  $S_0 = N_0 = 1.48 \times 10^{22} \text{ cm}^{-3}$ . Parameters of the diffusion coefficient of lead vacancies  $D_0 = 2.9 \times 10^{-5} \text{ cm}^2 \text{ s}^{-1}$  and  $E_D = 0.60 \text{ eV}$  [10] and the diffusion coefficient of interstitial lead atoms  $D_0 = 6.64 \times 10^{-2} \text{ cm}^2 \text{ s}^{-1}$  and  $E_D = 1.02 \text{ eV}$  [17]. Technological temperatures range from 600 K to 1300 K.

A system of equations describing the evolution of the concentration of Frenkel pairs, which considers the diffusion of each component, as well as their generation with the constant  $k_1$  and recombination with the constant  $k_2$ , has the following form [12,15]:

$$D_v \Delta V = k_1 S - k_2 VI, \quad (2)$$

$$D_i \Delta I = k_2 VI - k_1 S \quad (3)$$

where  $S$ ,  $I$ , and  $V$  are the volume concentrations of lead atoms at lattice sites, interstitial lead atoms, and vacancies,

respectively;  $k_2 = 4\pi\alpha D_i$ ,  $k_1 = k_2 V_0 I_0 / S_0$ . The formation time of the Frenkel pair is  $\tau = k_1^{-1}$ .

With the change of variables  $V = vV_0$ ,  $I = iI_0$ , and  $S = sS_0$ , the original system of equations will be rewritten in the following form:

$$\lambda_v^2 \Delta v = s - vi, \quad (4)$$

$$\lambda_i^2 \Delta i = vi - s, \quad (5)$$

where  $\lambda_v^2 = D_v / 4\pi\alpha D_i I_0$ ,  $\lambda_i^2 = 1 / 4\pi\alpha V_0$ . Taking the scale length  $l = \lambda_i$ , in the units of  $l$ , we will receive:

$$\gamma \Delta v = s - vi, \quad (6)$$

$$\Delta i = vi - s, \quad (7)$$

where  $\gamma = \lambda_v^2 / \lambda_i^2 = 10^{-3}$ .

From this system of equations, after summation, it follows that  $\gamma \Delta v + \Delta i = 0$ . Given that, at zero time, the relative concentrations are unit, we have:

$$\gamma v + i = \gamma + 1, \quad (8)$$

therefore



$$i = 1 + \gamma(1 - v). \quad (9)$$

The connection between  $s$  and  $v$  is as follows [12,15]:

$$V = V_0 \exp\left(\frac{\Delta E}{kT} \times \frac{s-s_0}{s_0}\right), \quad (10)$$

in dimensionless variables  $v = \exp(\alpha(s-1))$ , where  $\alpha$  is determined by the part of the vacancy formation energy that depends on the deviation of the concentration of lattice site atoms from the equilibrium value, and it is also determined by temperature. Therefore:

$$s = 1 + \frac{\ln(v)}{\alpha} \quad (11)$$

For small deviations,  $v = 1 + \delta v$ , the system of equations will be reduced to the equation of a harmonic oscillator for the concentration of vacancies in the coordinate space, and the solution will take the form:

$$v = 1 + \delta v_0 \cos\left(\frac{2\pi x}{\lambda}\right), \quad (12)$$

where  $\delta v_0$  is the amplitude of the initial deviation at the point  $x = 0$ , and  $\lambda$  is the spatial period of oscillations, which have to be estimated. The concentration of nodal atoms:

$$s = 1 + \frac{\delta v_0 \cos\left(\frac{2\pi x}{\lambda}\right)}{\alpha}, \quad (13)$$

and interstitial

$$i = 1 - \gamma \delta v_0 \cos\left(\frac{2\pi x}{\lambda}\right). \quad (14)$$

Substituting the approximate solutions into the differential equation for the concentration of vacancies, and leaving the terms with linear deviations from the equilibrium value, the period of spatial oscillations can be obtained as follows:

$$\lambda = \frac{2\pi}{\sqrt{\frac{1-\frac{1}{\alpha}}{\gamma}-1}}. \quad (15)$$

From the formula (15), we can see, that a significant impact on the period has  $\gamma$ . If  $\gamma \ll 1$  and  $\alpha > 1$ , then in dimensionless units:

$$\lambda \approx 2\pi\gamma^{1/2}. \quad (16)$$

That is, in the dimensional units:

$$\lambda \approx 2\pi\lambda_v = \sqrt{\frac{D_v\pi}{\alpha D_i I_0}} \quad (17)$$

If  $\gamma \rightarrow 1 - 1/\alpha$ , then  $\lambda \rightarrow \infty$ .

Figs. 5-6 show the results of calculations of the distribution period depending on the temperature and vacancy concentration for different energies  $\Delta E$ .

The solution of the system of equations by numerical methods confirms the received analytical solutions for small deviations at the crystallite boundary.

A strongly inhomogeneous interacting system with

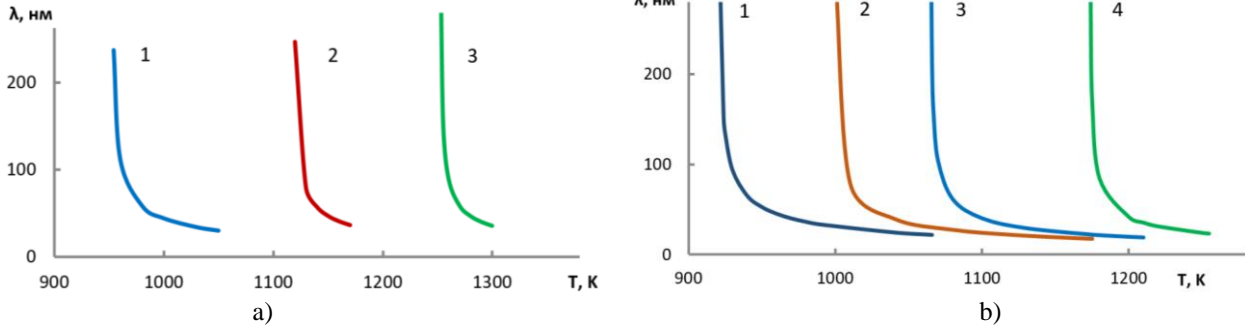


**Fig. 5.** Dependence of the period of oscillations on the technological temperature for: (a)  $\Delta E = 0.3$  eV, with vacancy concentration  $1 \cdot 10^{19} \text{ cm}^{-3}$  (1),  $2 \cdot 10^{19} \text{ cm}^{-3}$  (2), and  $3 \cdot 10^{19} \text{ cm}^{-3}$  (3); (b)  $\Delta E = 0.6$  eV, with vacancy concentration  $1 \cdot 10^{19} \text{ cm}^{-3}$  (1),  $1.5 \cdot 10^{19} \text{ cm}^{-3}$  (2),  $2 \cdot 10^{19} \text{ cm}^{-3}$  (3), and  $3 \cdot 10^{19} \text{ cm}^{-3}$  (4).

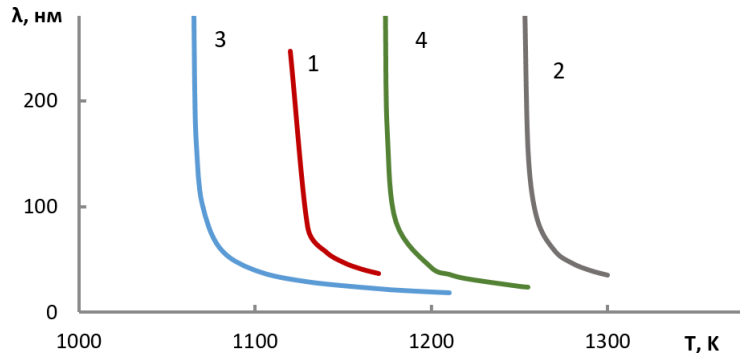


**Fig. 6.** Dependence of the period of oscillations on the technological temperature and vacancy concentration for  $\Delta E = 0.3$  eV (with vacancy concentration  $2 \cdot 10^{19} \text{ cm}^{-3}$  (1) and  $3 \cdot 10^{19} \text{ cm}^{-3}$  (2)) and  $\Delta E = 0.6$  eV (with vacancy concentration  $2 \cdot 10^{19} \text{ cm}^{-3}$  (3) and  $3 \cdot 10^{19} \text{ cm}^{-3}$  (4)).

diffusion can undergo a nonequilibrium phase transition. The system is open, it consumes vacancies formed from the outside media. The source of vacancies supports the existence of inhomogeneous structures. The described model was applied to describe the behavior of point defects in  $\text{Pb}_{1-x}\text{Sn}_x\text{Te}$ . The theoretical prediction suggests that the instability leads to inhomogeneous spatial structures and significant inhomogeneities in the distribution of interstitial lead atoms. Even if relatively small changes around 5 - 10% are observed, the concentration of interstitial defects changes remarkably, up to 2 - 3 times. This may have a crucial effect on the electrophysical properties of  $\text{Pb}_{1-x}\text{Sn}_x\text{Te}$  due to possible compensation effects. Areas depleted of interstitial lead are enriched in cationic vacancies and may have  $p$ -type of conduction, while the rest of the sample is  $n$ -type. In  $\text{Pb}_{1-x}\text{Sn}_x\text{Te}$ , the degree of compensation is usually quite high, which provides a low concentration of carriers. For example, small (approximately 0.1%) deviations from the homogeneous spatial distribution of donors can lead to significant (several times) differences in the Hall coefficient for two parts of one sample. As a result, the transition to the impurity type when the local concentration of interstitial tellurium atoms changes by 2-3 times is possible and the instability mechanism provides a natural explanation for the formation of  $n$ -type inclusions in  $p$ -type conductivity materials.

## Conclusions

In summary, the diffusion instability of the inhomogeneous distribution of lead in  $\text{Pb}_{1-x}\text{Sn}_x\text{Te}$  was

studied. A model for tellurium diffusion which includes two flows (fast interstitial defects and slow substitutions with preservation of lattice nodes) interacting with each other through cationic vacancies, is proposed. Vacancies may come, for example, from the surface, resulting in the fact, that their local concentration is always consistent with the local composition. For the exponential dependence of the concentration of vacancies on the composition, the homogeneous distribution can become unstable and turn into a certain inhomogeneous structure. With the available data for diffusion coefficients, it was found that the instability forms a layered structure with the concentration of internodal lead. Due to the presence of acceptor cationic vacancies, this observation can lead to the formation of internal  $p$ - $n$  junctions.

## Acknowledgements

The work was supported by the ESTEEM-3 H2020 EU-project, grant agreement No 823717 (AGH University of Science and Technology, Poland).

**Saliy Ya.** – Doctor of Physical and Mathematical Sciences, Professor;

**Nykyruy L.** – Ph.D., Professor, Head of Physics and Chemistry of Solids Department;

**Cempura G.** – Ph.D., Scientist in the Centre of Electron Microscopy for Materials Science;

**Soroka O.** – Ph.D, Associate Professor;

**Parashchuk T.** – Ph.D., Department of Inorganic Chemistry;

**Horichok I.** – Doctor of Physical and Mathematical Sciences, Professor.

- [1] I.V. Horichok, V.V. Prokopiv, R.I. Zapukhlyak, O.M. Matkivskyj, T.O. Semko, I.O. Savelikhina, T.O. Parashchuk, *Effects of oxygen interaction with PbTe surface and their influence on thermoelectric material properties*, J. Nano- Electron. Phys., 10(5) 05006 (2018); [https://doi.org/10.21272/jnep.10\(5\).05006](https://doi.org/10.21272/jnep.10(5).05006).
- [2] T. Parashchuk, I. Horichok, A. Kosonowski, O. Cherniushok, P. Wyzga, G. Cempura, A. Kruk, K.T. Wojciechowski, *Insight into the transport properties and enhanced thermoelectric performance of n-type  $\text{Pb}_{1-x}\text{Sb}_x\text{Te}$* , J. Alloys Compd. 860, 158355 (2021); <https://doi.org/10.1016/j.jallcom.2020.158355>.
- [3] R. Knura, T. Parashchuk, A. Yoshiasa, K.T. Wojciechowski, *Evaluation of the double-tuned functionally graded thermoelectric material approach for the fabrication of n-type leg based on  $\text{Pb}_{0.75}\text{Sn}_{0.25}\text{Te}$* , Appl. Phys. Lett. 119, 223902 (2021); <https://doi.org/10.1063/5.0075126>.
- [4] T. Parashchuk, L. Chernyak, S. Nemov, Z. Dashevsky, *Influence of Deformation on  $\text{Pb}_{1-x}\text{In}_x\text{Te}_{1-y}\text{Iy}$  and  $\text{Pb}_{1-x-y}\text{Sn}_x\text{In}_y\text{Te}$  Films*, Phys. Status Solidi B, 18, 1 (2020); <https://doi.org/10.1002/pssb.202000304>.
- [5] I.V. Horichok, M.O. Galushchak, O.M. Matkivskyj, I.P. Yaremij, R.Ya. Yavorskyj, V.S. Blahodry, O.I. Varunkiv, T.O. Parashchuk, *Thermoelectric Properties of Nanostructured Materials Based on Lead Telluride*, J. Nano- Electron. Phys. 9(5), 05022 (2017); [https://doi.org/10.21272/jnep.9\(5\).05022](https://doi.org/10.21272/jnep.9(5).05022).
- [6] B. Naidych, T. Parashchuk, I. Yaremij, M. Moyseyenko, O. Kostyuk, O. Voznyak, Z. Dashevsky & L. Nykyruy, *Structural and Thermodynamic Properties of Pb-Cd-Te Thin Films: Experimental Study and DFT Analysis*, Journal of Elec. Mater., 50, 580 (2021); <https://doi.org/10.1007/s11664-020-08561-5>.
- [7] Taras Parashchuk, Bartłomiej Wiendlocha, Oleksandr Cherniushok, Rafal Knura, and Krzysztof Wojciechowski, *High Thermoelectric Performance of p-Type PbTe Enabled by the Synergy of Resonance Scattering and Lattice Softening*, ACS Appl. Mater. Interfaces, 13, 41, 49027 (2021); <https://doi.org/10.1021/acsami.1c14236>.
- [8] L. Nykyruy, M. Ruvinskiy, E. Ivakin, O. Kostyuk, I. Horichok, I. Kisialiou, Y. Yavorskyj, A. Hrubyak, *Low-dimensional systems on the base of  $\text{PbSnAgTe}$  (LATT) compounds for thermoelectric application*, Physica E: Low-dimensional systems and nanostructures, 106, 10-18 (2019); <https://doi.org/10.1016/j.physe.2018.10.020>.
- [9] E.I. Rogacheva, O.N. Nashchekina, Y.O. Vekhov, M.S. Dresselhaus, S.B. Cronin, *Effect of thickness on the thermoelectric properties of PbS thin films*, Thin solid films, 423, 115 (2003); [https://doi.org/10.1016/S0040-6090\(02\)00968-9](https://doi.org/10.1016/S0040-6090(02)00968-9).
- [10] E.I. Rogacheva, T.V. Tavrtna, O.N. Nashchekina, S.N. Grigorov, K.A. Nasedkin, *Quantum size effects in PbSe quantum wells*, Applied Physics Letters, 80(15). 2690 (2002); <https://doi.org/10.1063/1.1469677>.

- [11] E.I. Rogacheva, O.N. Nashchekina, S.N. Grigorov, M.S. Dresselhaus, S.B. Cronin, *Oscillatory behavior of the transport properties in PbTe quantum wells*, Institute of Physics Publishing. Nanotechnology, 14, 53 (2003); <https://doi.org/10.1088/0957-4484/14/1/313>.
- [12] A.S. Vasin, M.I. Vasilevsky, *Simulation of diffusion instability of a mercury atomic distribution in the cadmium-mercury-tellurium alloy*, Phys. Solid State, 48, 37 (2006); <https://doi.org/10.1134/S1063783406010082>.
- [13] R. Knura, T. Parashchuk, A. Yoshiasa, K. T. Wojciechowski, *Origins of Low Lattice Thermal Conductivity of Pb<sub>1-x</sub>Sn<sub>x</sub>Te Alloys for Thermoelectric Applications*. Dalt. Trans. 50 (12), 4323 (2021); <https://doi.org/10.1039/d0dt04206d>.
- [14] Y.P. Saliy, R.S. Yavorskyi, *The redistribution modeling of implanted impurity stimulated by vacancies*, Materials Today: Proceedings, 35, 576 (2021); <https://doi.org/10.1016/j.matpr.2019.11.017>.
- [15] M.I. Vasilevskiy and E.V. Anda, *Diffusion instability of homogeneous distribution of mercury in cadmium mercury telluride*, Semicond. Sci. Technol. 10, 157 (1995); <https://doi.org/10.1088/0268-1242/10/2/006>
- [16] Krzysztof T. Wojciechowski, Taras Parashchuk, Bartłomiej Wiendlocha, Oleksandr Cherniushok, and Zinovi Dashevsky, *Highly efficient n-type PbTe developed by advanced electronic structure engineering*, J. Mater. Chem. C, 8, 13270 (2020); <https://doi.org/10.1039/D0TC03067H>.
- [17] Y.I. Ravich, B.A. Efimova, I.A. Smirnov, *Semiconducting Lead Chalcogenides*, Springer US, 1970. <https://doi.org/10.1007/978-1-4684-8607-0>.

Я. Салій<sup>1</sup>, Л. Никируй<sup>1</sup>, Г. Цемпура<sup>2</sup>, О.Сорока<sup>3</sup>, Т. Парашук<sup>2</sup>, І.Горічок<sup>1</sup>

## Періодичні наноструктури, індуковані точковими дефектами в Pb<sub>1-x</sub>Sn<sub>x</sub>Te

<sup>1</sup>Прикарпатський національний університет імені Василя Стефаника, Івано-Франківськ, Україна, [ihor.horichok@pnu.edu.ua](mailto:ihor.horichok@pnu.edu.ua)

<sup>2</sup>Університет науки та технологій AGH, Краків, Польща

<sup>3</sup>Івано-Франківський національний медичний університет Івано-Франківськ, Україна

Тверді розчини на основі телуридів свинцю та олова є відмінними кандидатами для створення віток р-типу провідності модулів термоелектричного генератора. Дослідження їх мікроструктурних властивостей є важливим питанням, оскільки дозволяє ефективно змінювати їхні електронні властивості та перенесення тепла. У даній роботі показано експериментальні залежності розподілу компонентів Pb<sub>1-x</sub>Sn<sub>x</sub>Te, які ідентифіковані як періодичні наноструктури із амплітудою  $\lambda \approx 50-500$  нм. Спостережувана періодичність пояснюється генерацією та рекомбінацією точкових дефектів внаслідок дифузійних процесів під час синтезу, спікання та відпалу зразків. Запропоновано модель, що описує утворення таких неоднорідностей у потрійних сполуках Pb<sub>1-x</sub>Sn<sub>x</sub>Te під час ізотермічного відпалу.

**Ключові слова:** точкові дефекти, наноструктури, PbSnTe.